"The Feasibility of a Cochlear Nucleus Auditory prosthesis based on microstimulation"

Contract No. NO1-DC-5-2105

QUARTERLY PROGRESS REPORT #10

Oct 1-Dec 31, 1997

HUNTINGTON MEDICAL RESEARCH INSTITUTES
NEUROLOGICAL RESEARCH LABORATORY
734 Fairmount Avenue
Pasadena, California 91105

D.B. McCreery, Ph.D.
T.G.H. Yuen, Ph.D.
L.A. Bullara, B.S.
W.F. Agnew, Ph.D.

HOUSE EAR INSTITUTE
2100 WEST THIRD STREET
Los Angeles, California 90057

ABSTRACT AND SUMMARY

These studies are a continuation of our program to determine safe and effective stimulus parameters for an auditory prosthesis based on multisite microstimulation in the ventral cochlear nucleus. Arrays of four discrete iridium microelectrodes, spaced 500 μm apart, were implanted into the posteroventral cochlear nucleus of adult cats.

One cat (cn122) was stimulated on 26 consecutive days, beginning 86 days after implantation of the array, using biphasic current pulses whose amplitude was modulated according to a logarithmically-compressed artificial voice signal. Each microelectrodes was pulsed at 250 Hz, and the stimulus was interleaved across the ensemble of microelectrodes. The protocol in this animal differed from that used in all previous cats, in that all 4 microelectrodes were pulsed. During the first three days of the regimen, only two of the microelectrodes were pulsed for 7 hours per day. On day 4, the remaining two microelectrodes were added, and henceforth each of the four was pulsed for 7 hours per day at 250 Hz , in the interleaved mode. On the day 23-26, the stimulation regimen was increased to 12 hours per day. The cat was sacrificed for histologic evaluation after the 26th session.

The electrical excitability of the neurons near the stimulating microelectrodes was assessed according to the changes in the recruitment characteristics of the compound evoked response recorded in the contralateral inferior colliculus. We generated the non-embedded recruitment characteristics from data acquired during low-frequency pulsing after each of the 7- or 12 hour sessions. The embedded curves were generated during (near the end of) the 7- or 12 hour sessions of stimulation from the pulses embedded in the artificial voice signal. The "non-embedded" and "embedded" recruitment curves each provide their own insights into the effects of the prolonged stimulation.

Thus, in cat 122, we were able to examine three phenomena: (1) The histologic effects, and the effects on neuronal excitability (both direct and transsynaptic) during 26 days of stimulation (2), the effects on neuronal excitability resulting from increasing

the number of pulsed microelectrodes in an ensemble of closely -spaced microelectrodes , and (3), the effects on neuronal excitability resulting from increasing the number of hours per day that the electrodes are pulsed.

Most of the physiologic effects of prolonged interleaved pulsing of closely-spaced microelectrodes were apparent by the end of the first day of the regimen . For the stimulus parameters used in this animal, there was mild depression of the electrical excitability of the neurons close to the microelectrodes, and the amount of depression varied slightly between microelectrodes. Overall, the effects were comparable to what we have seen in other animals stimulated for up to 15 days with these same parameters. There was a transient additional decrease of the excitability of neurons near microelectrode #1 where the two additional microelectrodes were added to the ensemble, but their excitability recovered after a few days. Lengthening the daily stimulation sessions (from 7 hours per day to 12 hours per day) had virtually no effect on neuronal excitability, and the directly- evoked, and transynaptically evoked components of the non-embedded or the embedded recruitment curves remained essentially unchanged. Over the 26 days of the stimulation regimen, the microelectrodes' access resistances, and their cathodic voltage transient (an index of their charge capacity) remained quite constant, and showed no clear trends.

The histological evaluations of the electrodes sites did not reveal any tissue injury that could be attributed to the prolonged electrical stimulation. There were no unpulsed control electrodes, but the neurons and neuropil near each of the 4 microelectrode tips appeared to be quite normal. The surrounding neuropil did not contain edematous axon segments, which is the cardinal feature of stimulation-induced tissue injury in the cochlear nucleus (McCreery et al, 1994). There was no evidence of healed micro-hemorrhages anywhere in the cochlear nucleus, a finding that continues to support the merits of blunt-tipped microelectrodes for chronic implantation and microstimulation. The only problem noted in the histologic evaluation was a localized inflammatory response near a segment of the upper shaft (but not at the tip) of microelectrode #3. This was probably due to a localized contaminant on the electrode

shaft. We are preparing to transfer part of our microelectrode fabrication to a clean-room, to reduce the chance of contamination of the uncured Epoxylite varnish by airborne particles.

METHODS

Fabrication of stimulating microelectrodes.

Activated iridium stimulating microelectrodes are fabricated from lengths of pure iridium wire, 50 μm in diameter. A Teflon-insulated lead wire is welded to one end of the iridium shaft, and the other end is shaped to a conical taper, by electrolytic etching. The microelectrodes have relatively blunt tips (a radius of curvature of approximately 6 μm) to reduce tissue injury during insertion into the brain. The entire shaft and wire junction then is coated with 3 thin layers of Epoxylite 6001-50 heat-cured electrode varnish. The insulation is removed from the tip by dielectric destruction, leaving an exposed geometric surface area of approximately 1000 μm^2. The individual electrodes are assembled into an integrated array of 4 microelectrodes spaced approximately 400 μm apart. The integrated array, with its closely-spaced microelectrode shafts, is designed to approximate the dimensions of an array that can be implanted into the human posteroventral cochlear nucleus using a tool inserted through the translabyrinthine surgical approach to the CP angle.

The iridium electrodes are "activated" to increase their charge capacities, soaked in deionized water for 120 hours, and sterilized with ethylene oxide.

Implantation of stimulating and recording electrodes

Young adult cats are anesthetized with Pentothal sodium, with transition to a mixture of nitrous oxide and Halothane. Implantation of the electrodes is conducted using aseptic surgical technique. The cat's head is placed in a stereotaxic frame, and the skull is exposed as far back as the posterior fossa by reflecting the scalp and muscles. A pair of stainless steel recording electrodes is implanted by stereotaxis into

the right inferior colliculus through a small craniectomy. The compound action potential induced by a train of clicks delivered to the left ear is used to position the recording electrodes.

A small craniectomy is made in the posterior fossa over the cerebellum, through which the array of iridium stimulating electrodes is inserted by stereotaxis into the left posteroventral cochlear nucleus (PVCN). Since the feline cochlear nucleus lies on the lateral surface of the brainstem and the human cochlear nucleus is buried behind the middle cerebellar peduncle, the feline array of 4 mm microelectrodes was inserted through a portion of the overlying cerebellar flocculus, so that we could evaluate electrodes whose length was appropriate for use in humans. The microelectrodes were positioned first by stereotaxic coordinates and the final positioning was achieved by observing the compound potential evoked in the inferior colliculus while stimulating with the microelectrode.

Stimulation protocols and data acquisition

For the prolonged stimulation regimen, we have simulated an acoustic environment with a computer-generated artificial voice The artificial voice reproduces many of the characteristics of real speech, including the long-term average spectrum, the short-term spectrum, the instantaneous amplitude distribution, the voiced and unvoiced structure of speech, and the syllabic envelope. The artificial voice signal is then passed through a full wave rectifier and then undergoes logarithmic amplitude compression, before being sent through an appropriate anti-aliasing filter. The amplitude of the signal from the filter then sets the amplitude of the charge-balanced stimulus pulses which are delivered to each electrode at 250 Hz, in an interleaved manner. The range of spike amplitudes is shifted so that acoustic silence is represented by a stimulus amplitude of 6 μA, which is close to the response threshold of the neurons near the tip of the properly functioning microelectrodes. The maximum amplitude of the stimulus pulses was set to 20 μA. Thus, the maximum charge per phase was 3 nC. The nominal geometric surface area of the microelectrodes was 1000

μm^2, so the maximum charge density was 300 $\mu C/cm^2$. During the stimulation, the electrodes were held an anodic bias of approximately 350 mV, with respect to an implanted Ag/AgCl reference electrode.

The artificial voice signal was presented for 15 seconds followed by 15 seconds in which the stimulus amplitude was held at 6 μA (near the threshold of the evoked response). This 50% duty cycle is intended to simulate a moderately noisy acoustic environment. Stimulation and data acquisition was conducted using the two-way radiotelemetry stimulation and data acquisition system described previously (QPR # 4, Contract NO1-NS-2-2323). This telemetry system and its companion software allows continuous monitoring of the voltage waveform across the stimulating microelectrodes, and of the compound evoked potential induced in the inferior colliculus by the stimulating microelectrodes. The access resistance of each microelectrode was calculated as Ra=e/i, where I the amplitude of the current pulse, and e is the nearly instantaneous voltage transient at the leading edge of the electrode voltage transient that develops in response to the current pulse. The cathodic voltage transient, Vac, is then calculated as the portion of the total electrode voltage transient, minus the access voltage (I x RA). It represents the polarization of the electrode interface during the cathodic phase of the cathodic-first pulse pair, and is a measure of the electrode's charge capacity (lower Vac at a particular current) indicates higher charge capacity)

At intervals after implantation, and before and after each daily session of stimulation, the recruitment curves of the evoked responses were recorded in the inferior colliculus. The responses evoked by 1024 to 4096 consecutive charge-balanced, controlled-current stimulus pulses applied to the stimulating microelectrodes were averaged to obtain an averaged evoked response (AER). For each AER, the amplitude of the first and second component was measured after the averaged response is filtered through a low-pass filter with a bandpass of 250 Hz to 2.5 kHz. The amplitude of the early and second components is measured from the peak of the positivity on the leading edge to the trough of the subsequent negativity (Figure 1). The response growth function (recruitment curve), which represents the recruitment

of the excitable neural elements surrounding the microelectrode, is generated by plotting the amplitude of the first or second component of each of several AECAPs against the amplitude of the stimulus pulse that evoked the responses.

The conventional (non-embedded) recruitment curves were generated before and immediately after the sessions of prolonged stimulation. The stimulus frequency was 50 Hz, which is much lower than during the 7-hour test session. In addition, a limited number of "embedded" recruitment curves were acquired during the first or last 45 minutes of some of the 7- or 12 hour sessions of stimulation from the pulses comprising the 250 Hz, amplitude-modulated pulse train . This procedure, which requires approximately 45 minutes per microelectrode, was described in detail in QPR #5. Briefly, when the appropriate pulse amplitude (e.g., 6 μA) is generated by the artificial voice, subsequent stimulus pulses are suspended for 10 msec, which is long enough for the first and second components of the evoked response to be recorded in the inferior colliculus. Pulsing at the full stimulus rate then resumes, and the computer waits 150 msec before resuming its search for the next 6 μA pulse, at which time another evoked response is recorded. This is repeated until the required number of responses to 6 μA has been collected and averaged, and the process is repeated for each of 7 stimulus amplitudes.

The conventional (non-embedded) recruitment curves allow detection of depression of neuronal excitability that persists after the termination of the high-rate stimulation with the artificial voice signal. If it is severe, this type of depression may persist for several days. Changes in the non-embedded recruitment curves identify stimulation protocols that place significant stress on the neurons of the lower auditory system. The embedded recruitment curves, in contrast, allows us to determine how the regimen of prolonged stimulation affects the neuronal response to the actual artificial voice signal. The non-embedded and embedded responses, and the histologic evaluation of the implant sites, provide complementary data on the safety and efficacy of the stimulation regimen.

Within 15 minutes after the end of the last day of stimulation, the cats were

deeply anesthetized with pentobarbital and perfused through the aorta with ½ strength Karnovsky's fixative (2.5% glutaraldehyde, 2% paraformaldehyde and 0.1M sodium cacodylate buffer). The cochlear nucleus and adjacent portion of the brainstem were resected, embedded in paraffin, sectioned serially in the frontal plane (approximately parallel to the shafts of the stimulating microelectrodes) at a thickness of 8 μm, and stained with Cresol Violet (Nissl stain) or with hematoxylin and eosin.

RESULTS

Physiologic findings (CN122.)

The 26-day stimulation regimen was begun 86 days after implantation of the microelectrodes into the ventral cochlear nucleus. Figure 1 shows an average evoked response from Microelectrode #1 in the left PVCN , and recorded in the right inferior colliculus. There is a large first and second component in the AECAP. The first component begins less than 1.2 msec after the stimulus, and therefore it is assumed to represent neural activity evoked directly in the cochlear nucleus neurons that project to the inferior colliculus. The second component probably represents the post-synaptic excitation of neurons in the inferior colliculus. The presence of large direct and transsynaptic components in the responses evoked from two of the microelectrodes in cat CN122 allows us to compare the effects of the various manipulation of the stimulation regimen on the direct electrically excitability of the neurons in the PVCN, and also their effects on the efficacy of synaptic transmission in the lower auditory system.

Electrodes 1 and 3 were pulsed for 7 hours/day on each of the first 3 days of the 26-day regimen, using a 250 Hz pulsing rate, modulated according to the artificial voice signal, and with a 50% duty cycle as described above. .

Figure 2 shows the effect of pulsing 2 microelectrodes, and then the effect of increasing the number of pulsed electrodes (from 2 to 4) on the excitability of neurons near microelectrode #1 (one of the two microelectrodes that were pulsed throughout the entire 26-day regimen). Figure 2A shown the effect on the direct response, and

figure 2B shows the effect on the transsynaptic response. For microelectrode #1, most of the persisting effects of the stimulation (a small increase in the threshold of the non-embedded evoked response) were evident by the end of the first 7 hours of stimulation. The effect of the stimulation on the second component (the transsynaptic response) of the evoked response is no greater than the effect on the direct response, indicating that the effects are attributable to a depression of the electrical excitability of the neurons in the PVCN that are excited directly by the electrical stimulation,rather than to a reduction in the efficay of the synptic transmission. On the 4th day, the addition of microelectrodes 2 and 4 to the ensemble of pulsed electrodes did induce a small decrease in the slope (the rate of growth) of the directly- evoked response (Figure 2A), and this effect is also seen in the transsynaptic response, as we would expect. This effect of the additional electrode was transitory, and by the end of the 19th day of pulsing, the recruitment of the direct response evoked from electrode #1 was very similar to what it had been after the first day of pulsing. Figure 3A and 3B show the corresponding results for microelectrode #3, (the other microelectrode that was pulsed throughout the entire regimen). Here, however, there was slightly less depression of neuronal excitability than was the case for microelectrode #1. By the end of the 19th day, the effects of the long regimen were quite similar for both microelectrodes.

The recruitment curves generated from the non-embedded responses provide a good indication of the amount of persisting depression of neuronal excitability at the end of each daily session of stimulation, and hence, they are an index of the amount of stress that is imposed on the neurons of the PVCN by the stimulation regimen. The responses generated from the stimulus pulses embeded in the artificial voice pulse sequence are probably a better indication of the effects of the stimulation on the threshold and growth of the percepts that would be invoked by the artificial voice signal. Unfortunately, the high data throughput rate (250 Hz per electrode × 4 electrodes = 1000 p.p.s.) caused a timing error in the custom computer software, and during the first four days of the protocol, the data for the embedded responses was missorted. This problem was remedied on the fifth day. Figure 4 shows the non-

embedded and embedded recruitment curves of the early (directly evoked) component of the response from microelectrode #3. As in previous animals, the growth (slope) of the embedded response lagged behind the non-embedded response over the mid-range of the artificial voice signal, but the threshold of both responses was approximately 6 μA. Note that the embedded response did not change significantly between the 5th and 19th day of pulsing.

Extending the length of the daily stimulation sessions had virtually no effect on the recruitment curves of either the non-embedded or embedded responses. Figure 5A and 5B shows the non-embedded recruitment of the direct and transsynaptic components of the response evoked from electrode #1 at the end of the 22nd day (the last day of pulsing for 7 hours per day) and after the 26th day (the 4th day in which the electrodes were pulsed for 12 hours per day). Figure 6 shows the corresponding results for the direct component of the response evoked from microelectrode #3. Figure 7 shows the embedded recruitment curves of the direct response evoked from microelectrode #3. In all cases, extending the length of the daily sessions had very little effect on the threshold and growth of the response.

Electrode performance

Figure 8A shows the access resistance of the 4 microelectrodes during the 26-day stimulation regimen. The access resistances of electrode 1 and 3 were obtained just before the start of the first day of pulsing (indicated as "day 0" on the plots) . Figure 8B shows the cathodic voltage transient for each of the 4 electrodes. The access resistance and voltage transients of electrode 1 were low, although the threshold of the evoked response from this electrode was comparable the other electrodes. The geometric surface area of its tip may have been greater than the nominal value of 1000 μm^2. Over the 26 days of the stimulation regimen, the access resistance of all 4 microelectrode remained quite constant, and showed no clear trends. Their cathodic voltage transient (an index of their charge capacity) tended to increased over the first 22 days of the regimen, but the process that was responsible for this

gradual decrease in charge capacity was not irreversible, since the transients on three of the electrodes decreased on day 23. On day 23 we did experience some problems with an intermittently broken battery cable in the telemetry pack. The stimulator contains protective circuity to limit the voltage transient during such mishaps, and the outputs are capacitively coupled to protect the electrodes and tissue , and there were no discernable histologic or physiologic consequences of this mishaps. However, it is likely that the electrode's anodic bias underwent an unknown number of brief transients, which may have been sufficient to "clean" the iridium oxide on the electrode's active surface.

In summary, most of the physiologic effects of prolonged interleaved pulsing of closely-spaced microelectrodes were apparent by the end of the first day of the regimen . For the stimulus parameters used in this animal, there was mild depression of the electrical excitability of the neurons close to the microelectrodes, and the amount of depression varied slightly between microelectrodes. Overall, the effects were comparable to what we have seen in other animals stimulated for up to 15 days with these same parameters. There was a transient additional decrease of neuronal excitability near microelectrode #1 where two additional microelectrodes were added to the pulsed ensemble. Extending the length of the daily stimulation sessions (from 7 hours per day to 12 hours per day) had virtually no effect on either the directly evoked, or transynaptically evoked components of either the non-embedded or the embedded recruitment curves.

Histologic findings

Figure 9A show an oblique section through the lower segment of the track and the site of the tip of microelectrode #1 (bar=50 μm). The tip was in the ventral part of the central nucleus of the PVCN, just dorsal to the confluence of myelinated fibers that forms the trapezoid body. The electrode track is surrounded by a compact glial sheath approximately 10 μm in thickness. The surrounding neuropil is compact and appears to be healthy. There is no infiltration of inflammatory cells. Figure 9B shows the site of

the tip (T) at higher magnification (bar=25 μm). There are several multipolar neurons close to the tip. These neurons are slightly more densely stained than are the multipolar neurons farther from the tip, but otherwise appear to be normal.

Figure 10A and 10B show the lower track and site of the tip of microelectrode #2, near the medial margin of the PVCN and near the upper boundary of the trapezoid body, and approximately 350 μm lateral to the track of microelectrode #1. The lower part of the tract of the Epoxylite-insulated electrode shaft, is surrounded by a compact glial sheath less than 10 μm in thickness. In this histologic section, there are few neurons closest to the tip, but the adjacent neuropil appears to be compact and healthy.

Figure 11A shows the lower portion of the track and the site of the tip of microelectrode #3 (Bar = 100 μm) . Figure 11B shows the site of the tip of the microelectrode at higher magnification (Bar=25 μm). The track is surrounded by a compact glial sheath approximately 10 μm in thickness, and the surrounding neuropil is compact and appears to be normal. There is no infiltration of inflammatory cells. Several multipolar neurons very close to the site of the tip appear normal and are not hyperchromic to the Nissl stain. There are no perineuronal haloes. In Figure 11A, the arrow indicates the site of a localized inflammatory reaction, farther up on the shaft. Figure 11C shows an oblique section through the track , and through the site the reaction (bar=50 μm). Lymphocytes surround a nearby blood vessel (perivascular cuffing) and other lymphocytes have infiltrated the glial sheath surrounding the track. The sheath itself is thickened and the surrounding neuropil appears slightly edematous. This is the only site at which this type of localized inflammatory reaction was seen in animal CN122. It is notable that these microelectrodes had been implanted for 109 days at the time the animal was sacrificed. The reaction may have been provoked by a contaminant on the electrode shaft.

Figures 12A and 12B shows track and the site of the tip of microelectrode #4 (Bar= 50 μm and 25 μm, respectively). The neuropil adjacent to the track and near the site of the tip is compact, and there is no edema or infiltration of inflammatory cells.

Multipolar neurons, some as near as 15 μm from the tip, appear to be normal and are indistinguishable from the neurons farther from the tip.

II: Long-term stability of microelectrodes in the cats' cochlear nucleus (cn74).

Our contract calls for us to implant stimulating microelectrodes into the cochlear nuclei of animals for at least 4 months and to monitor their performance over this interval. In our current studies, we allow at least 60 days (typically 90 to 120 days) to elapse after implantation of the stimulating electrodes, before initiating the stimulation protocols. However, four animals (cn41, cn42, CN74 and CN107) were reserved as long-term subjects in order to monitor the long-term stability of the chronically-implanted microelectrodes.

We have also continued to follow the performance of stimulating microelectrodes that have been implanted in cat cn74 for more than 1650 days, and in cat cn107, for more than 600 days. Both microelectrodes are still functioning well. Figure 13A and 13B show the recruitment curves of the response evoked in the PVCN of cat CN74 by microelectrode #1 and #2, and recorded in the inferior colliculus. These curves were acquired at various times between 14 and 1653 days after implantation of the microelectrodes. The threshold and the slope of the recruitment curves of the evoked response have remained quite stable. This confirms our earlier findings that the connective tissue capsule around the tips of these microelectrodes does not continue to thicken over time, and also demonstrates that there are no large changes in the number or excitability of neurons and axons in the tissue surrounding the site of the electrode tip, since for microelectrode #1, the threshold of the evoked response actually decreased over time, and there was little change in the slope of the recruitment curve (a function of the number of neurons excited) . The low threshold of the electrically- evoked response also confirms that the tip of the stimulating microelectrode has remained within the PVCN through the 1653 days in situ

DISCUSSION

Previously, we have demonstrated that intranuclear microstimulation allows an orderly access to the tonotopic organization of the posteroventral cochlear nucleus in the cat. (McCreery et al, 1998). We have shown that it should be possible to convey at least 4 separate channels of acoustic information into the cochlear nucleus using microelectrodes spaced 300-500 μm apart along the dorsoventral axis. In human subjects, 4 channels appears to be sufficient for good intelligibility of speech (Shannon et al, 1997). The data presented in this report indicates that at least 4 closely-spaced microelectrodes can be safely pulsed in the interleaved mode, using a stimulation regimen that model what an implant patient might encounter. Pulsing 4 closely-spaced electrodes does not seriously degrade the performance of the individual electrodes, and that it does not increase the risk of stimulation-induced tissue injury.

REFERENCES

McCreery, D.B, , T.G.H. Yuen, W.F. Agnew and L.A. Bullara (1994) Stimulation parameters affecting tissue injury during microstimulation in the cochlear nucleus of the cat Hearing Research 77:105-115, .

McCreery, D.B. Shannon R.V., Moore J.K, Chattegee, M. (1998) Accessing the tonotopic organization of the ventral cochlear nucleus by intranuclear microstimulation (Submitted to IEEE-Trans. Reheb .Eng.)

Shannon, R.V. , F. Zeng, V. Kamath, J. Wygonski, and M. Ekelid, "Speech recognition with primarily temporal cues," *Science,* vol. 270, pp. 303-304, 1995.

Response evoked by 20 μA pulses in cochlear nucleus and recorded in contralateral inferior colliculus

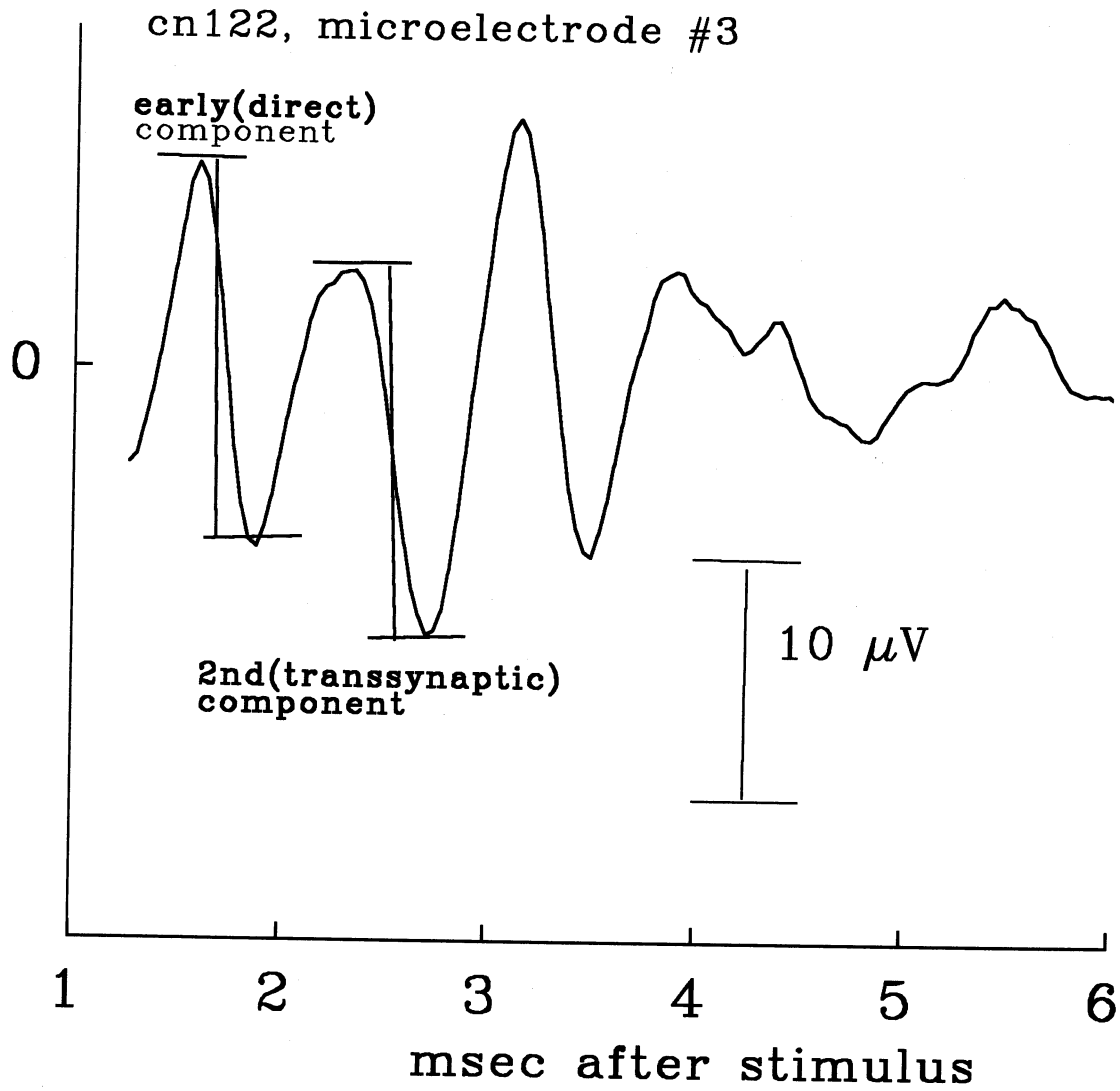

cn122tra.spq

Figure 1

Electrodes 1&3, then 1,2,3,4 pulsed 6–60 μA, 250 Hz, 50% duty cycle, 7 hrs/day

Non–embedded response from electrode #1

Effect, on direct response, of pulsing 2 electrodes, then adding 2 more

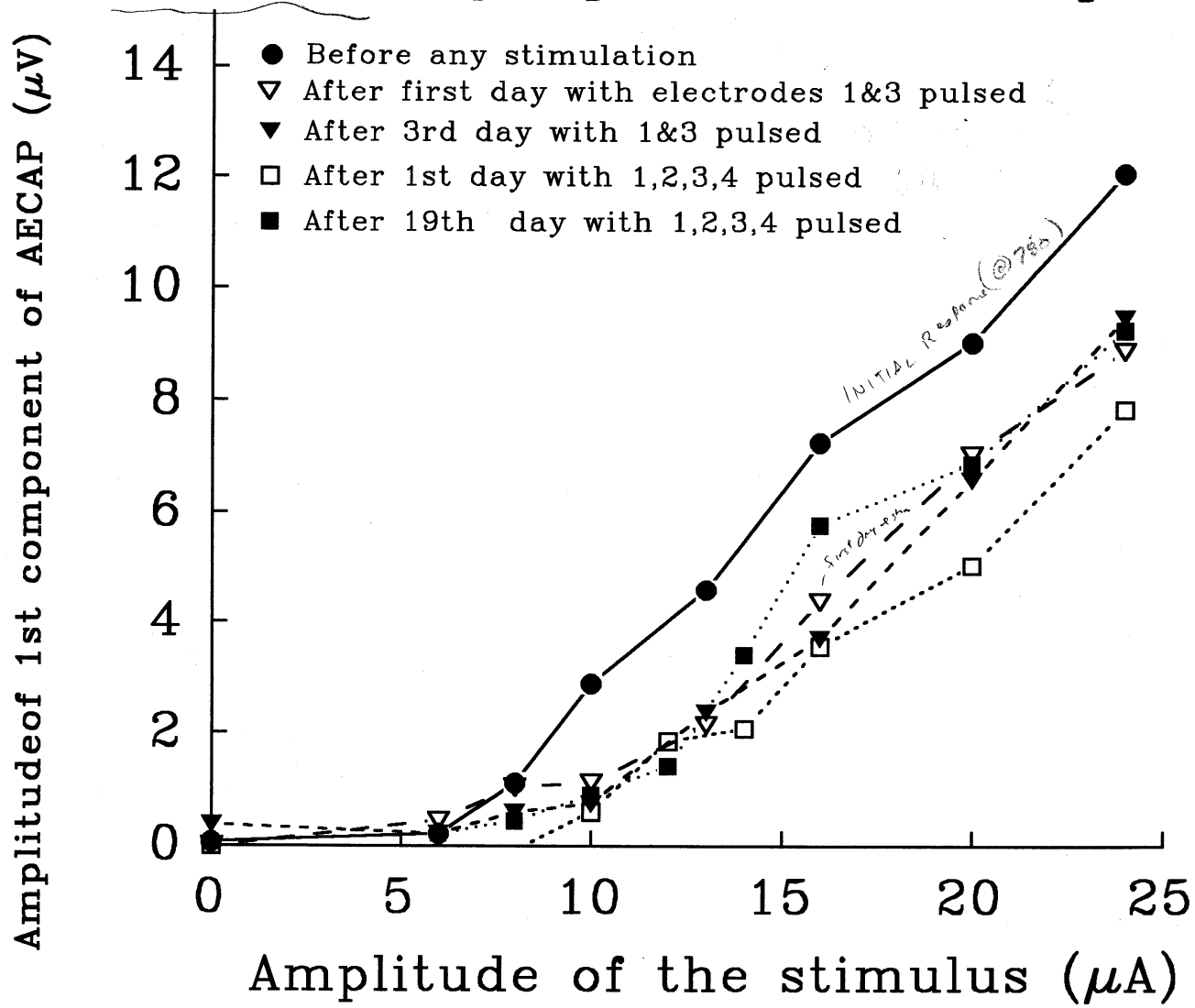

cq122z1.spg

Figure 2A

Electrodes 1&3, then 1,2,3,4 pulsed 6–20 μA, 250 Hz, 50% duty cycle
Non–embedded response from electrode #1

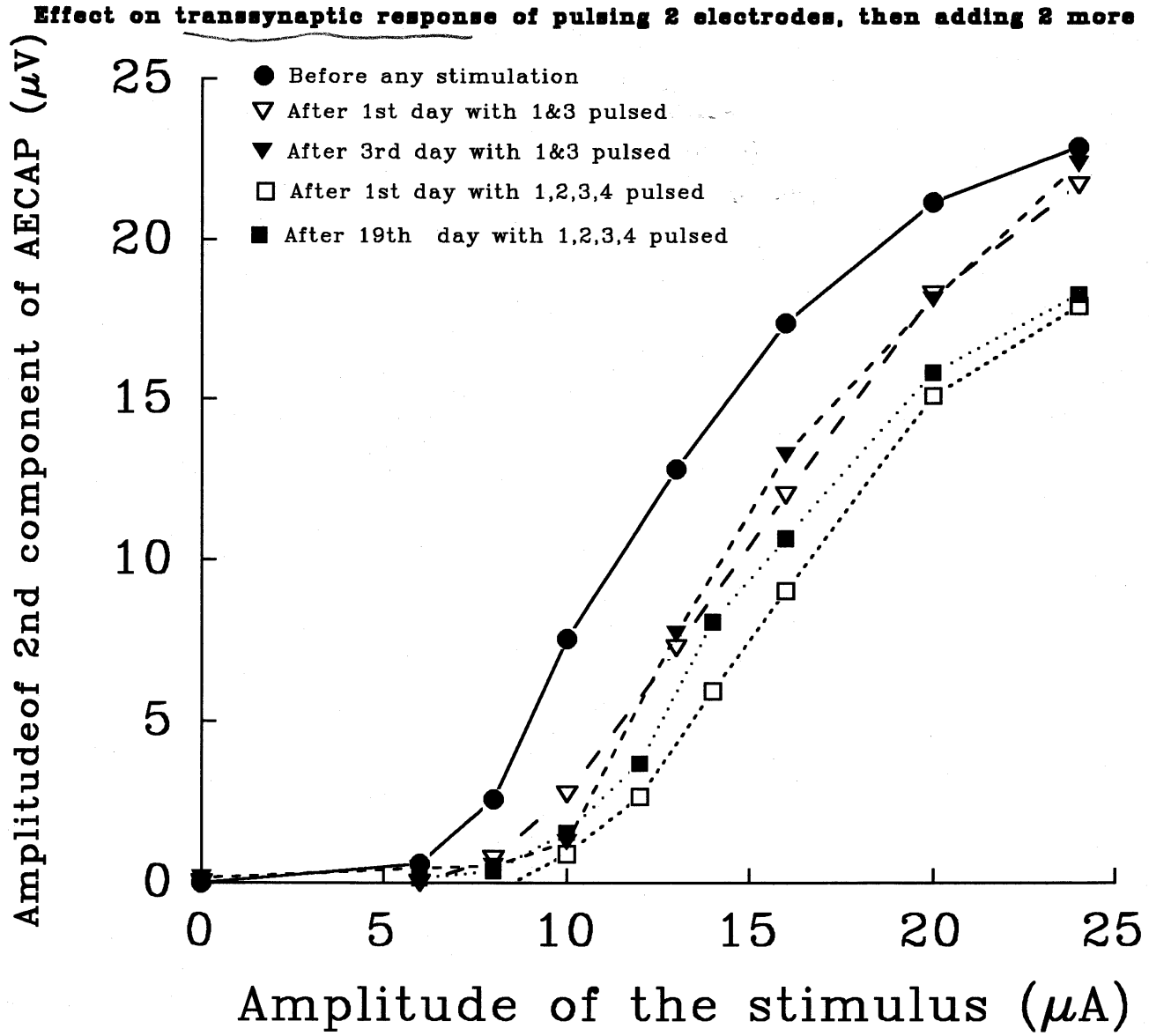

cq122t1.spg

Figure 2B

Electrodes 1&3, then 1,2,3,4 pulsed 6–20 μA, 250 Hz, 50% duty cycle
Non–embedded response from electrode #3,

Effect on direct response of pulsing 2 electrodes, then adding 2 more

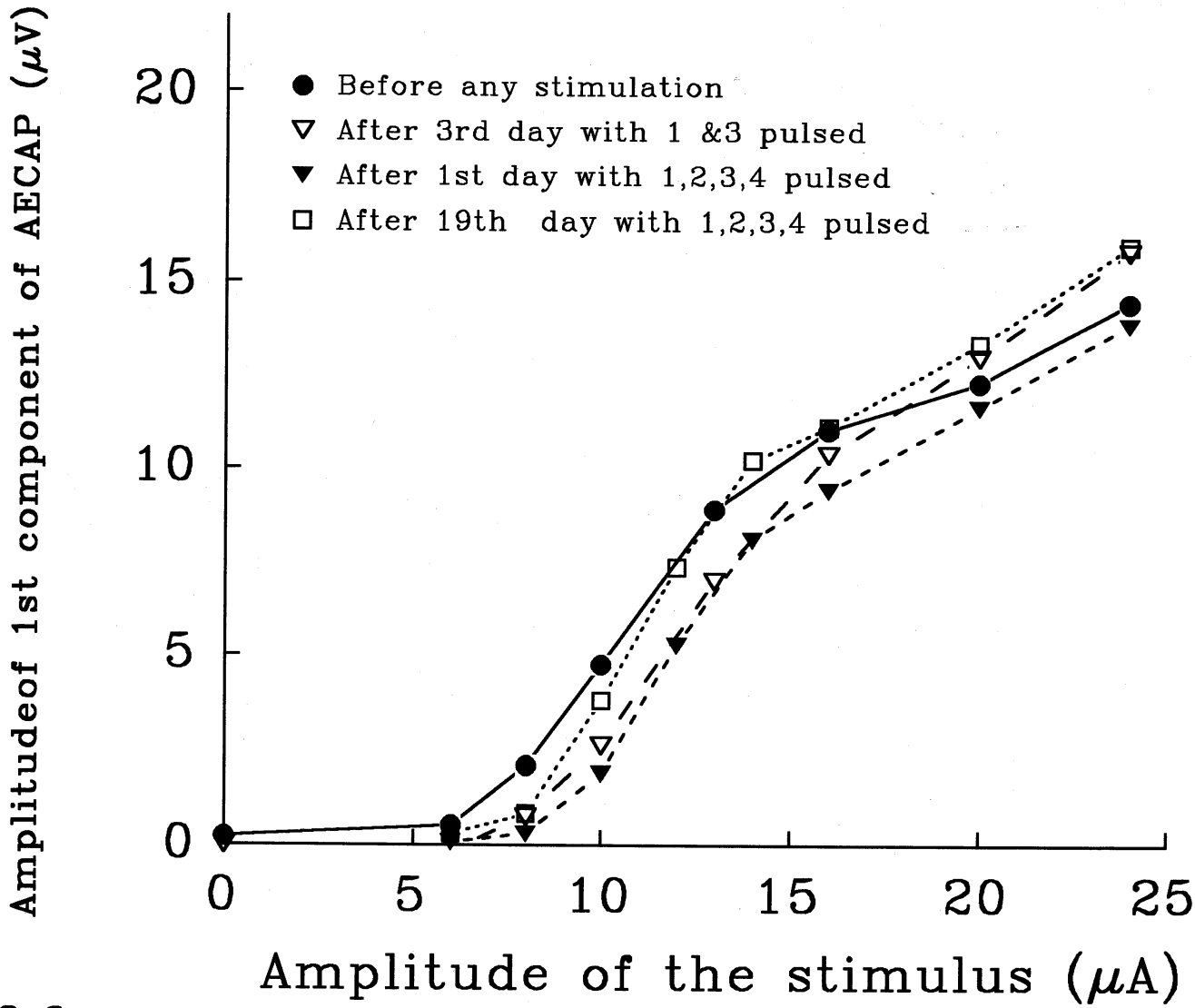

cq122z3.spg

Figure 3A

Electrodes 1&3, then 1,2,3,4 pulsed 6−20 μA, 250 Hz, 50% duty cycle
Non−Embedded response from electrode 3

Effect on transynaptic response of pulsing 2 electrodes, then adding 2 more

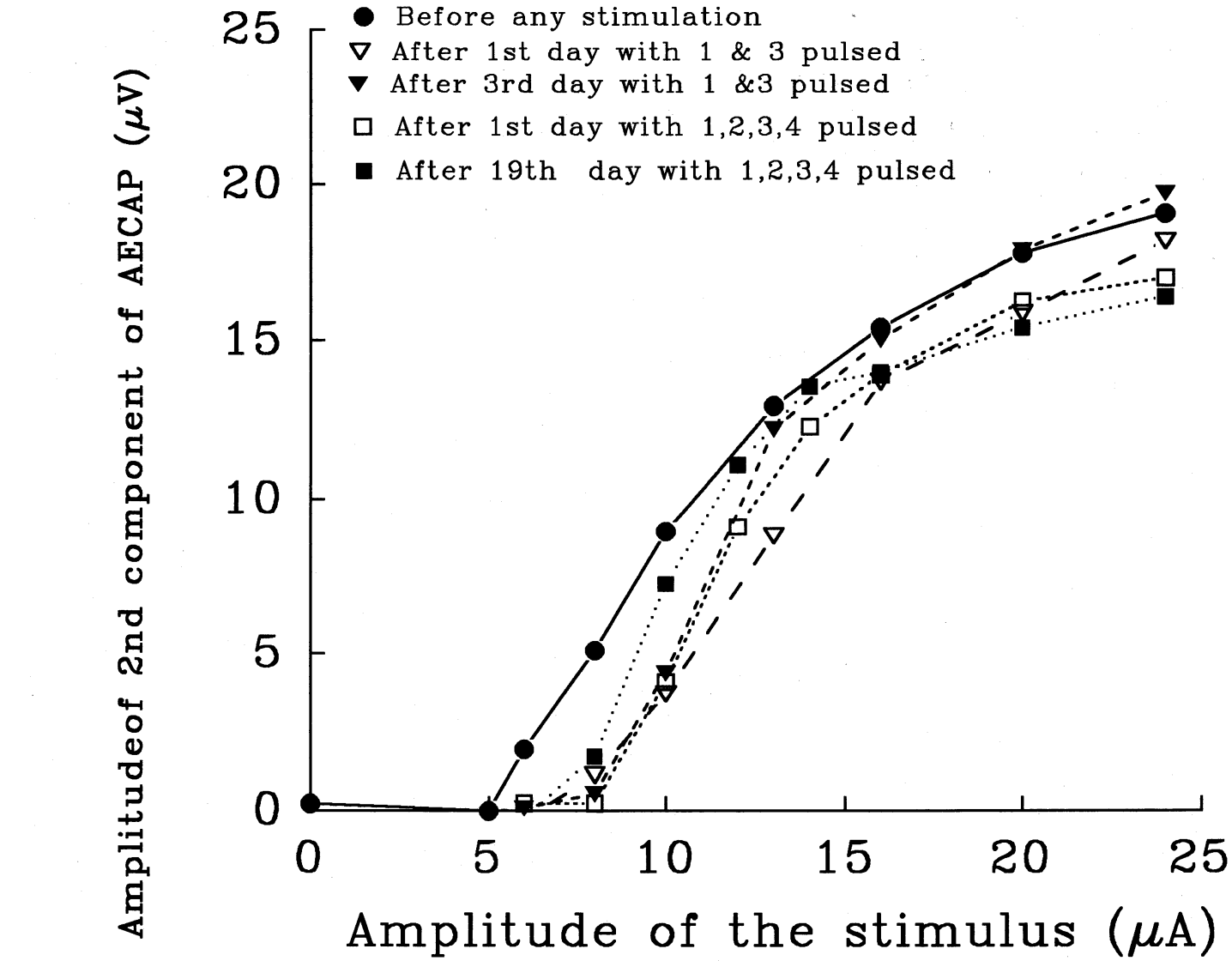

cq122t3.spg

Figure 3B

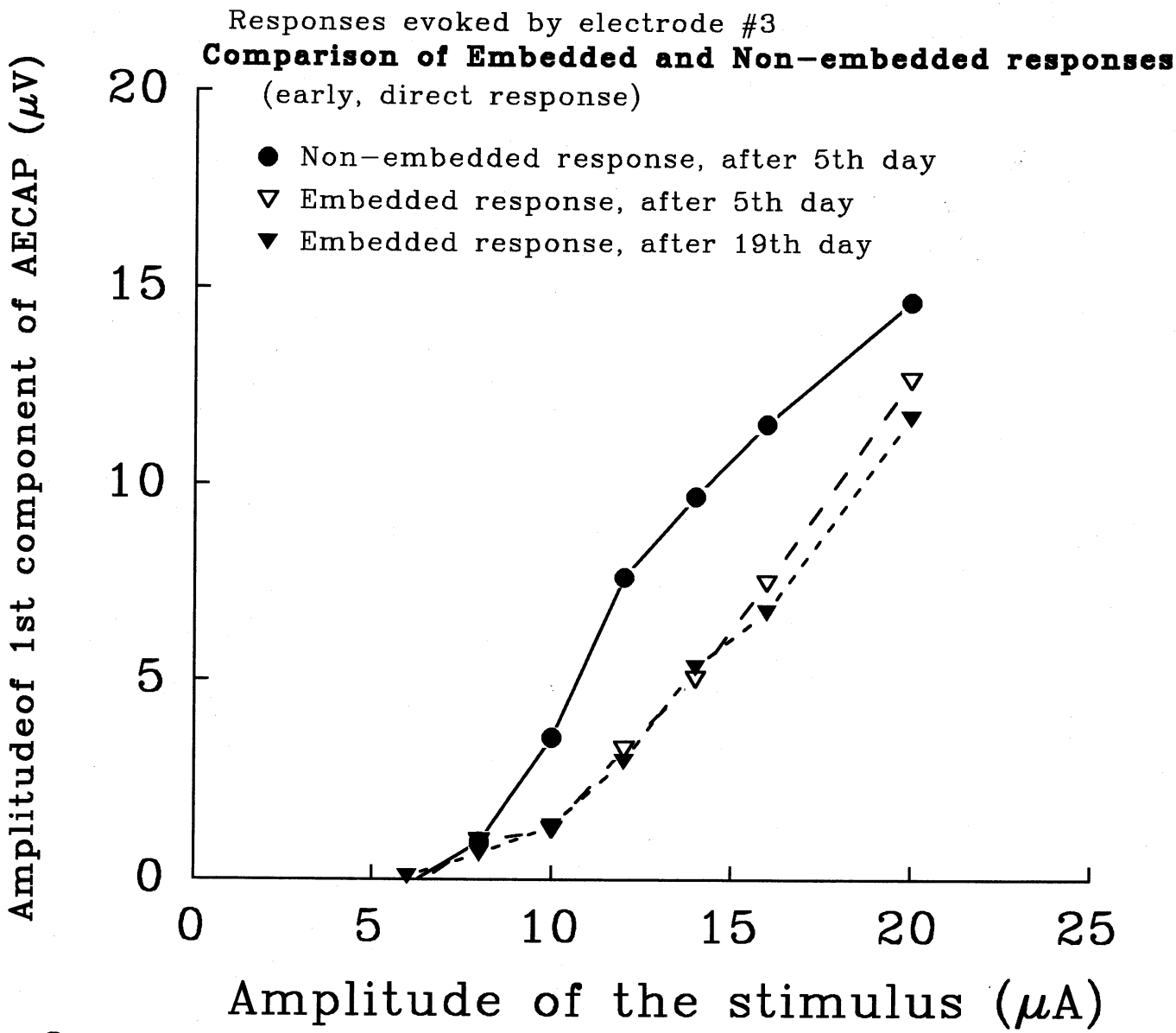

cq122ze3.spg

Figure 4

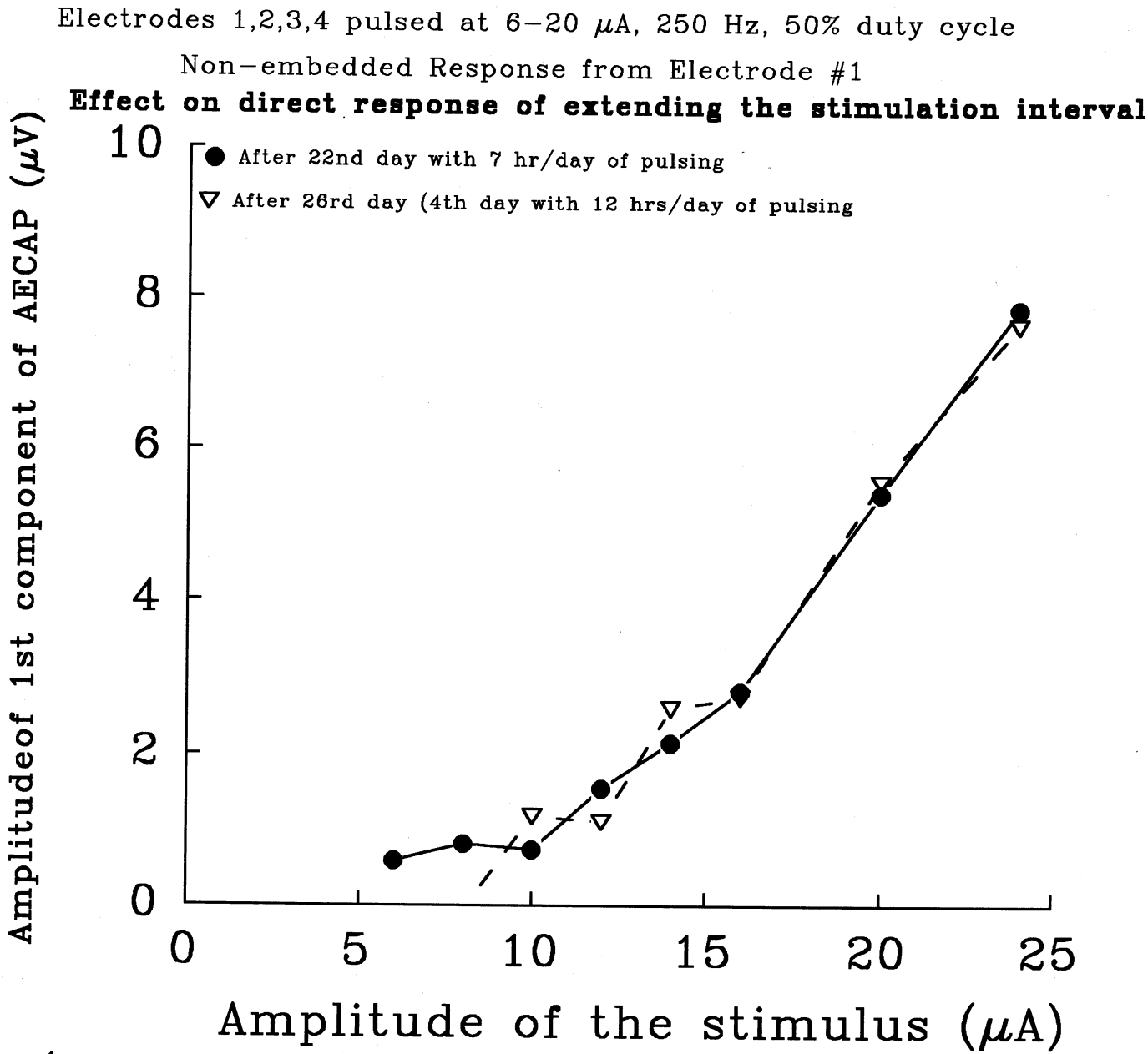

cq122ez1.spg

Figure 5A

Electrode 1,2,3,4 pulsed at 6–20 μA, 250 Hz, 50% duty cycle
Non–embedded response evoked from electrode #1
Effect on transsynapic response of extending the stimulation interval

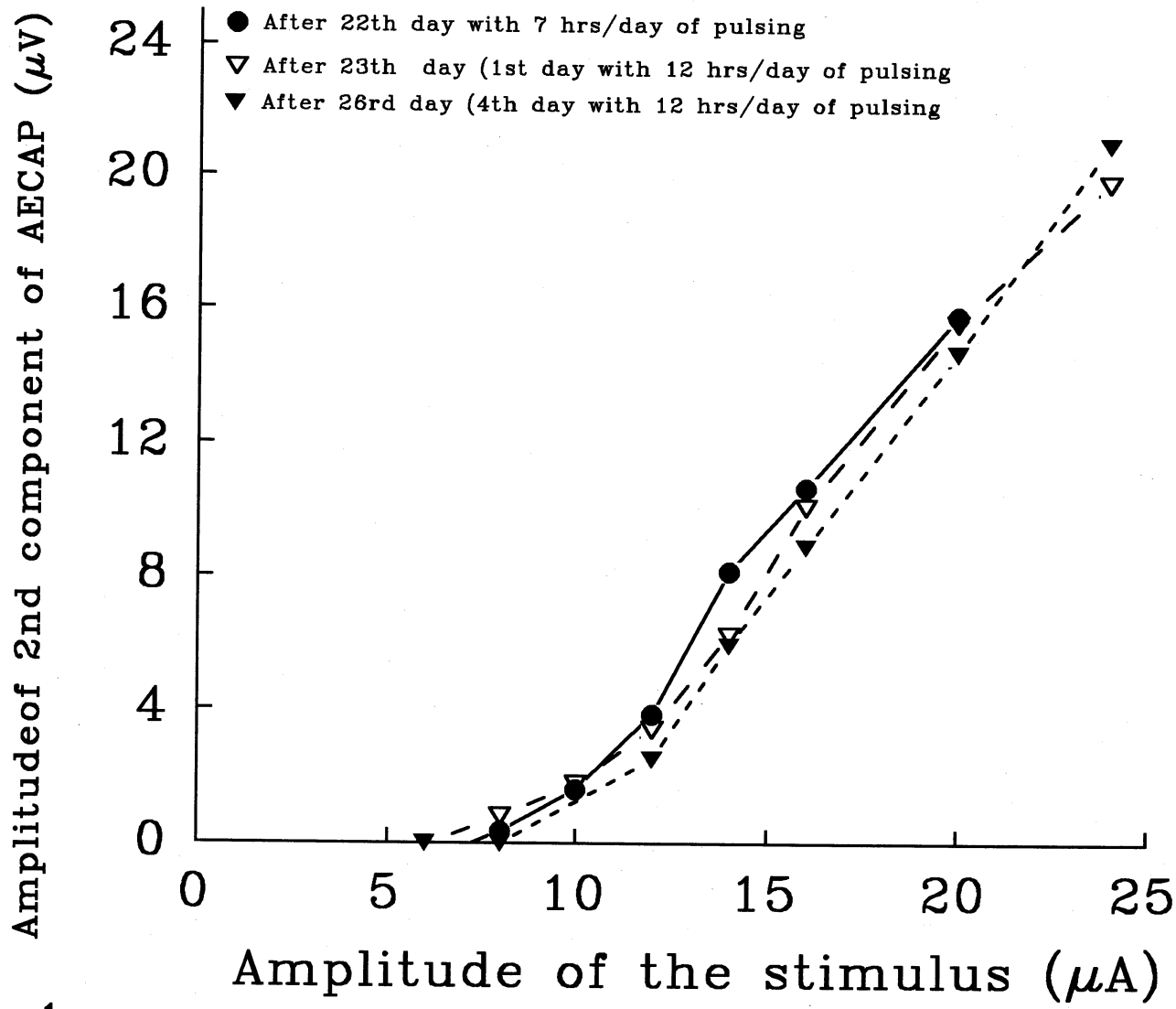

cq122ee1.spg

Figure 5B

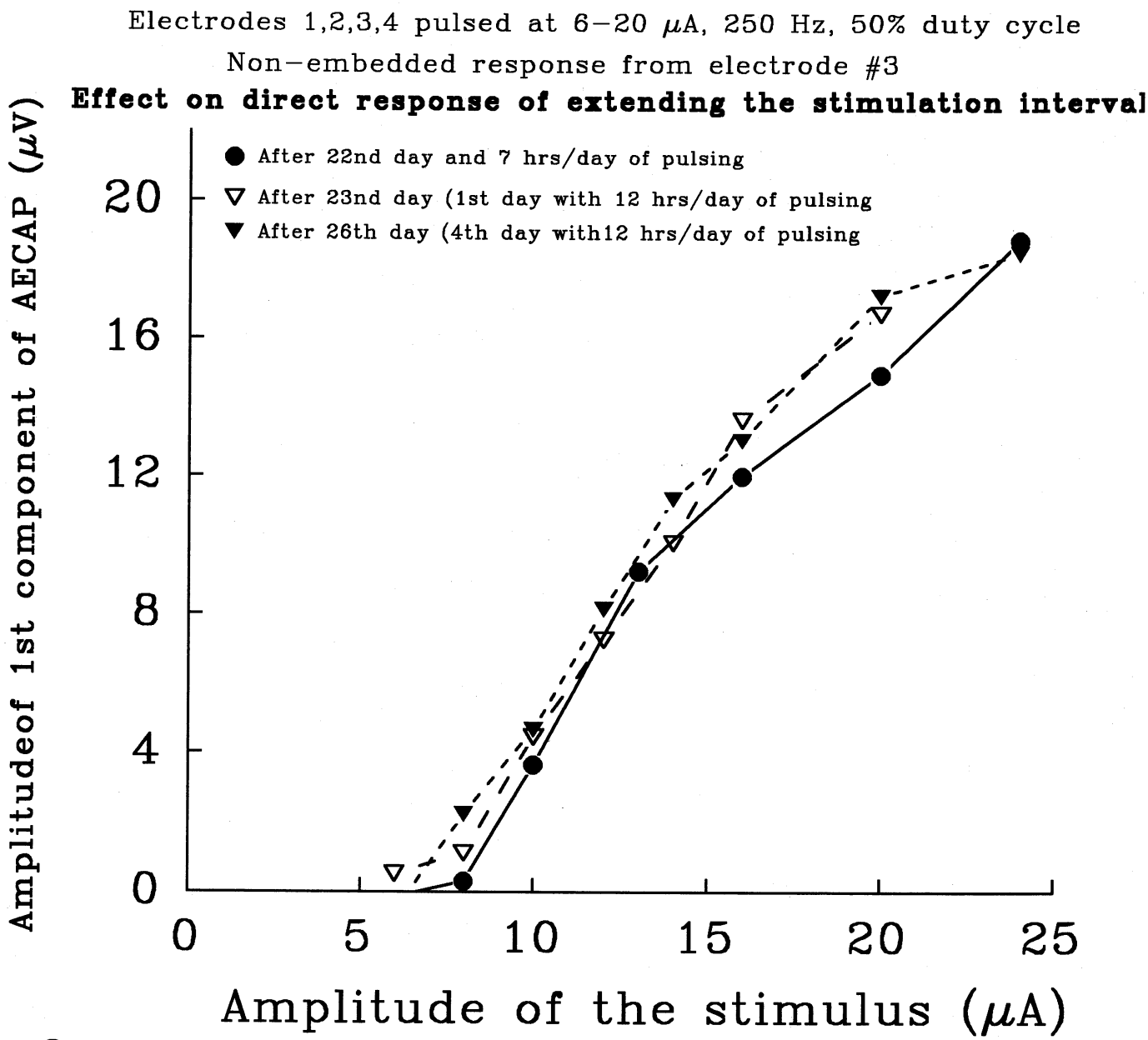

cq122ez3.spg

Figure 6

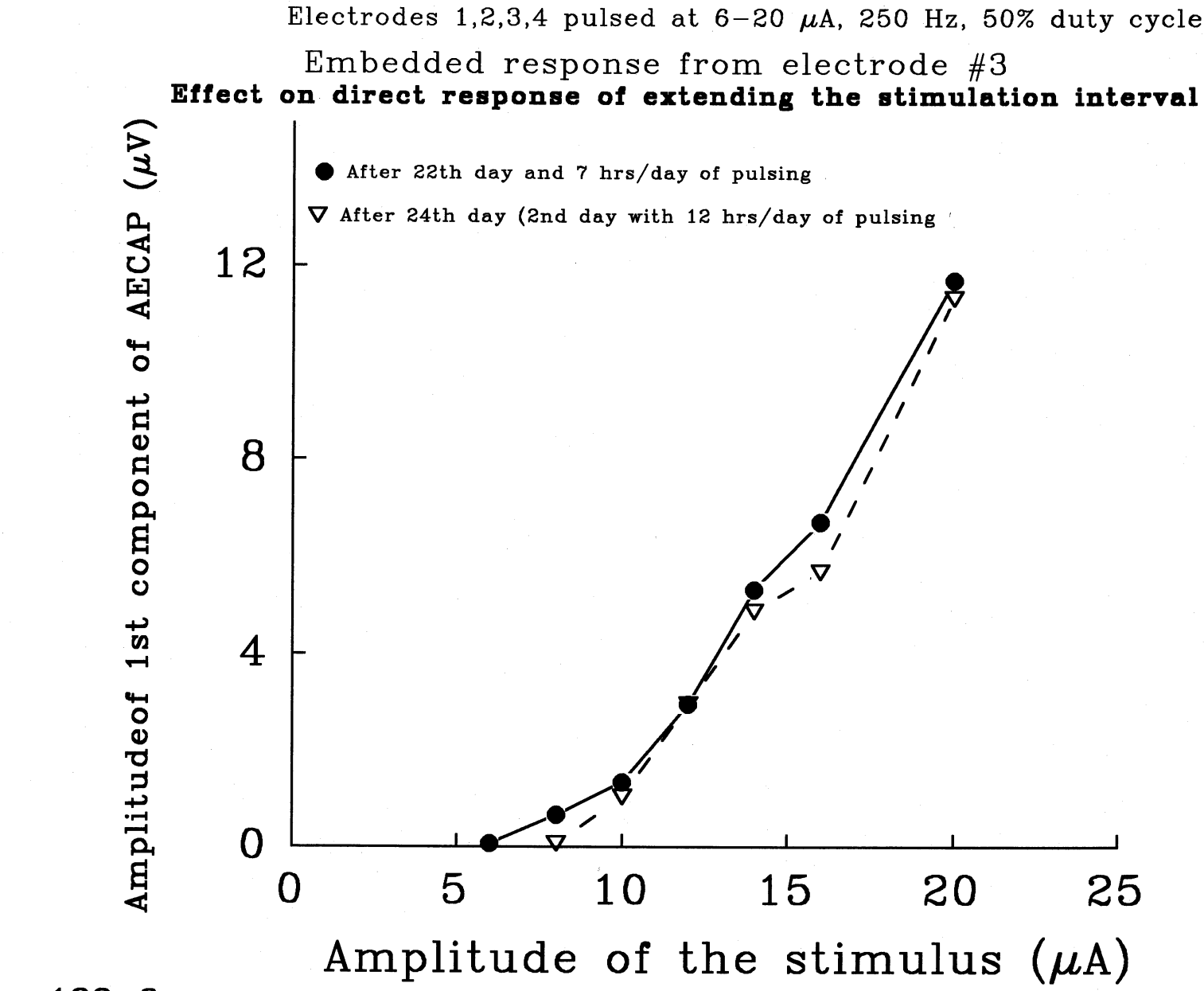
Electrodes 1,2,3,4 pulsed at 6–20 μA, 250 Hz, 50% duty cycle
Embedded response from electrode #3
Effect on direct response of extending the stimulation interval
After 22th day and 7 hrs/day of pulsing
After 24th day (2nd day with 12 hrs/day of pulsing
Amplitudeof 1st component of AECAP (μV)
0
4
8
12
0
5
10
15
20
25
Amplitude of the stimulus (μA)
cq122w3.spg

Figure 7

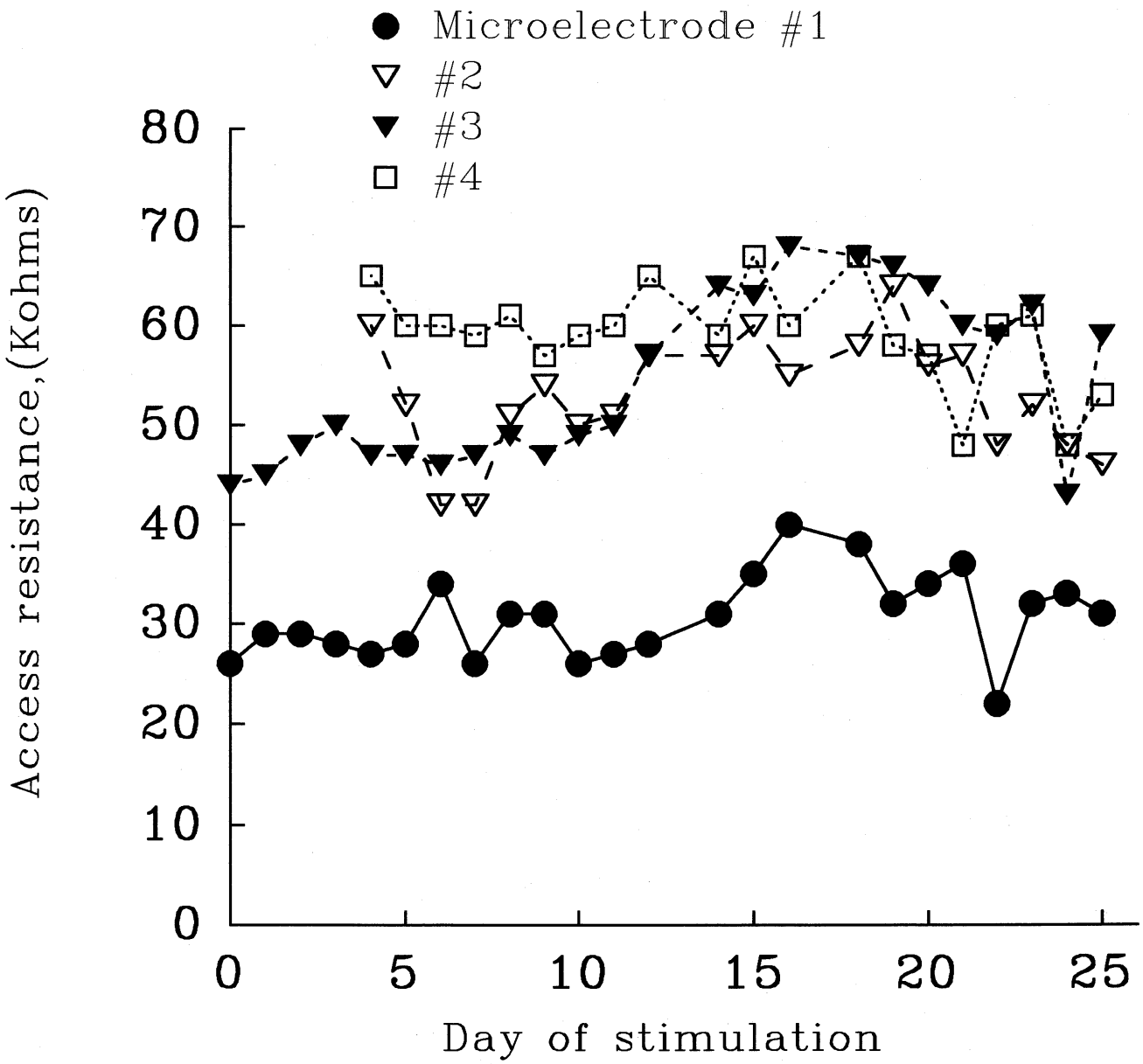

cn122rac.spg

Figure 8A

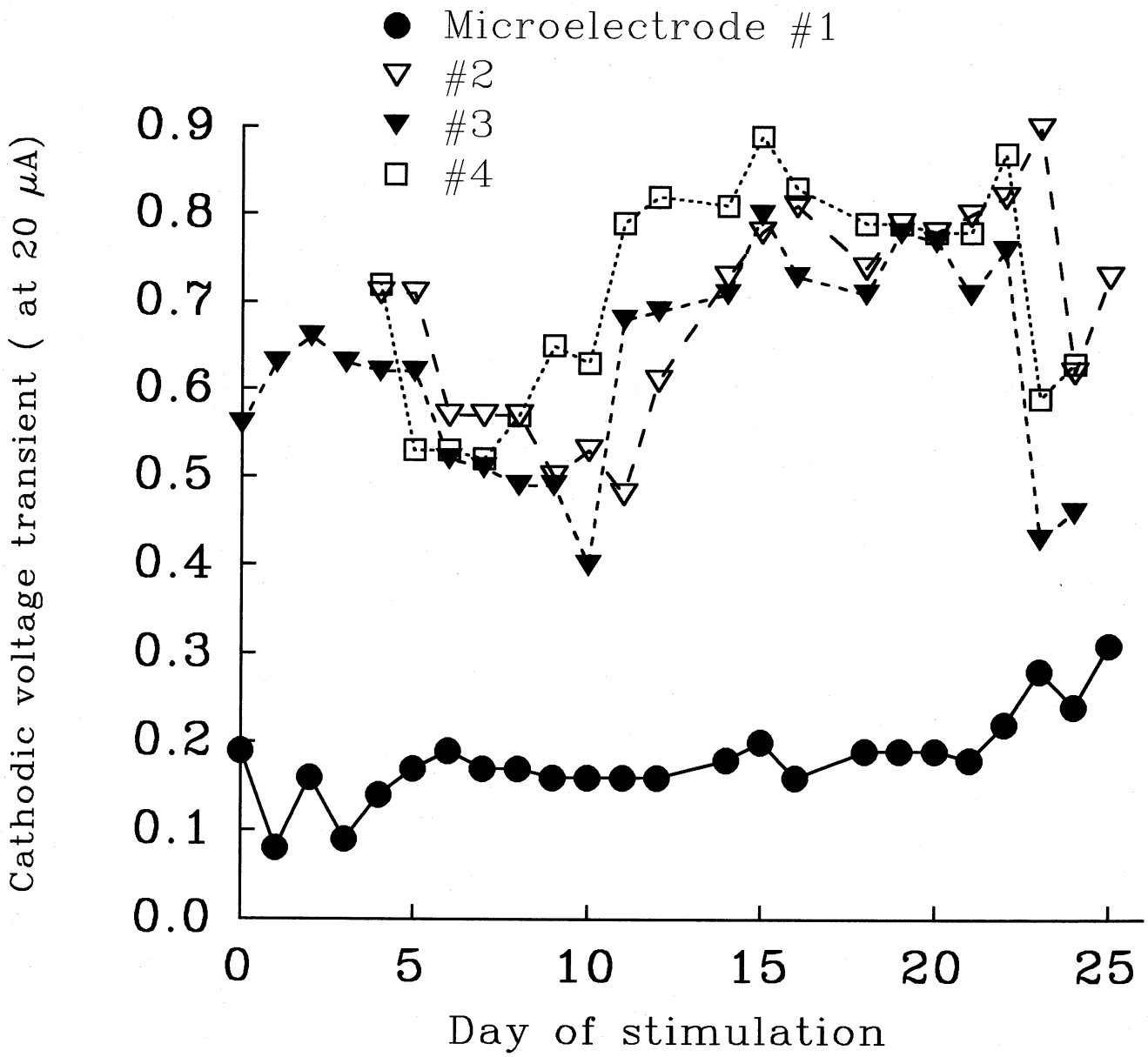

cn122cvt.spg

Figure 8B

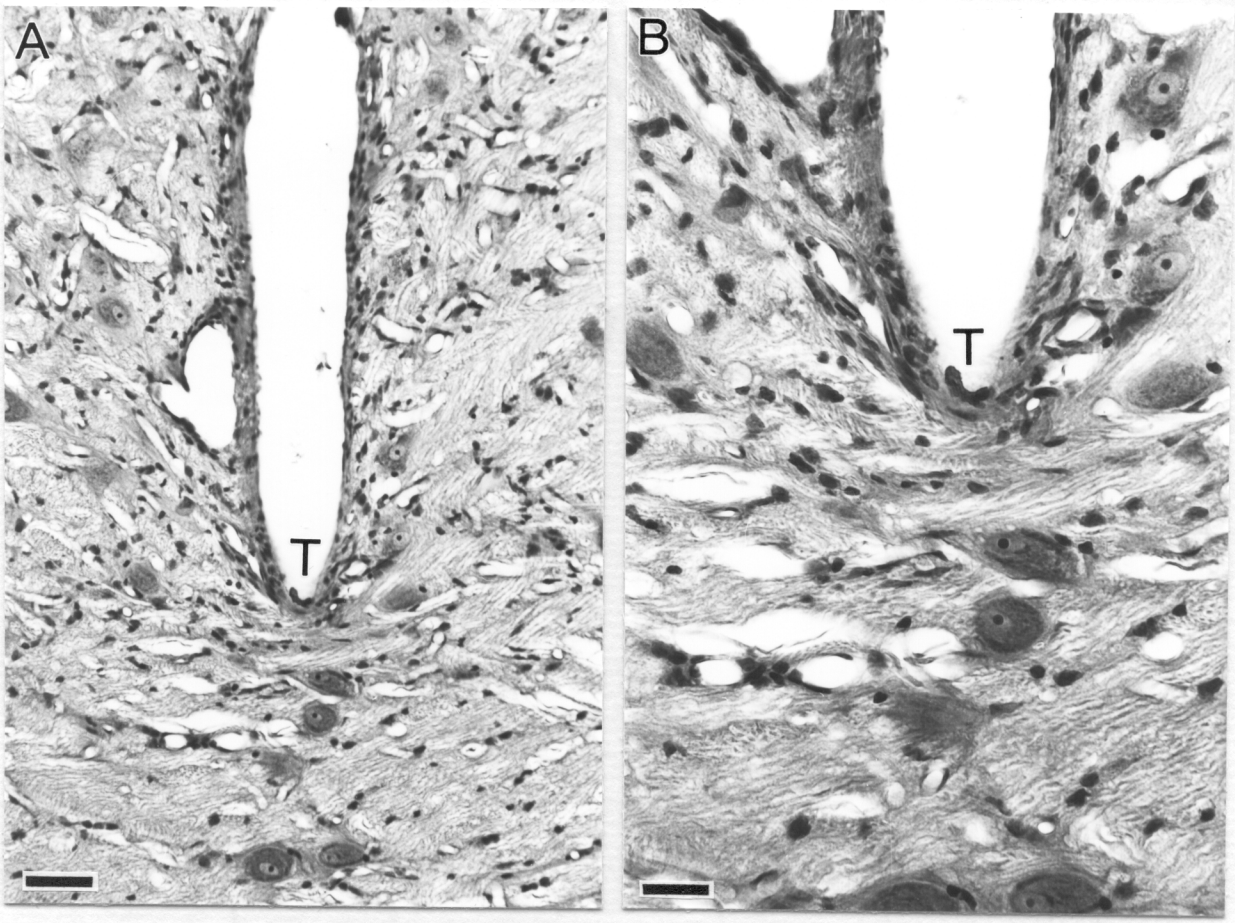

Figure 9

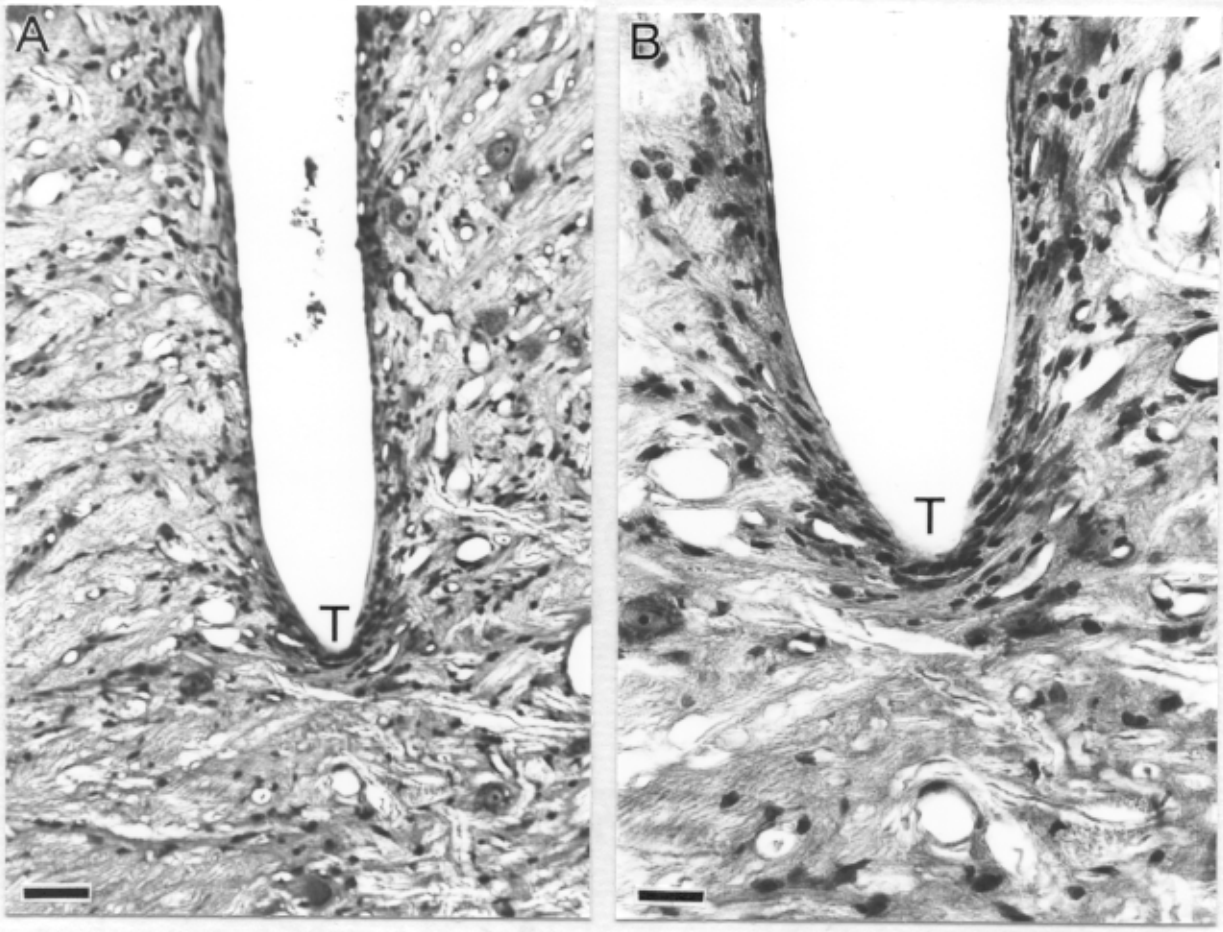

Figure 10

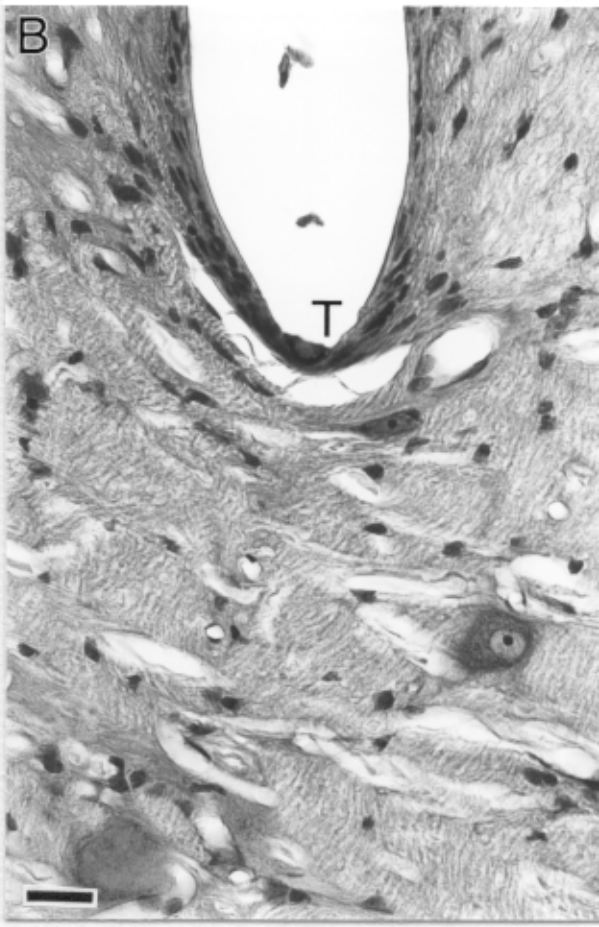

Figure 11

Figure 11C

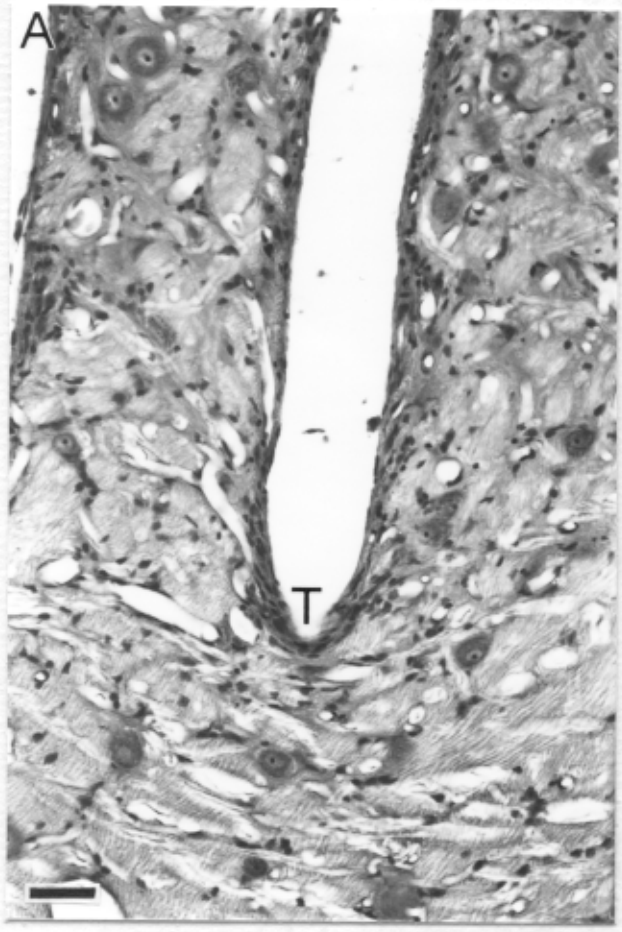

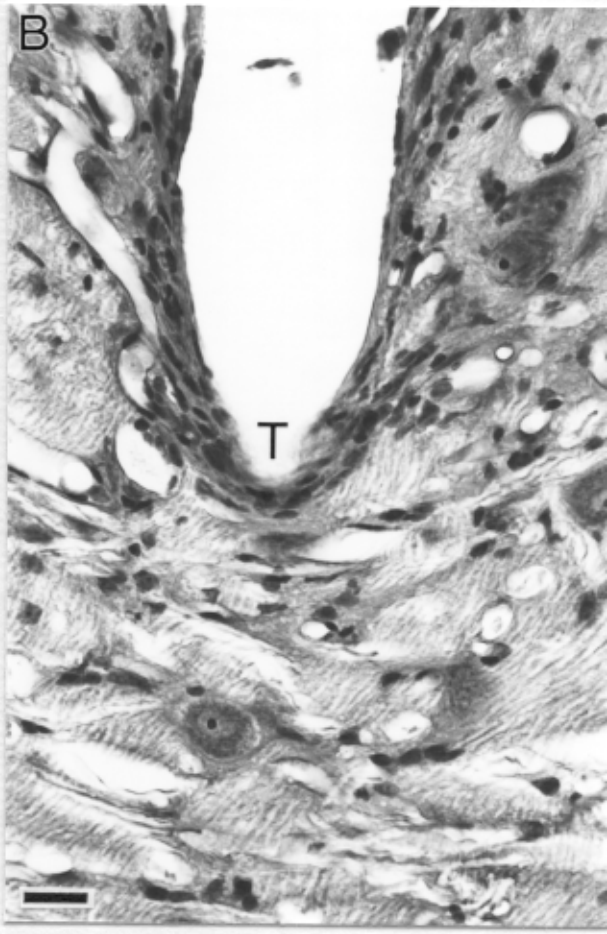

Figure 12

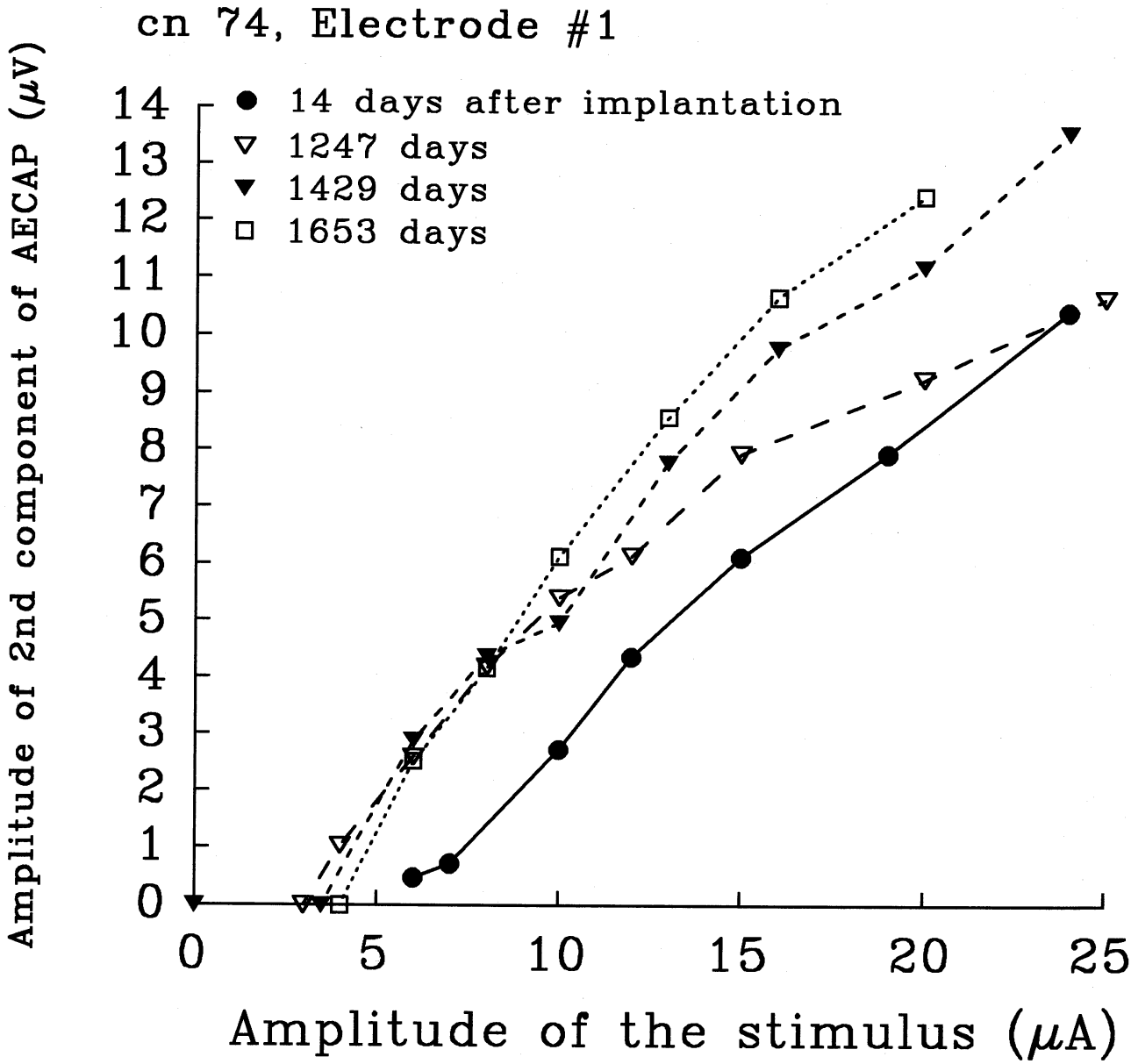

cnq74wb2.spg

Figure 13A

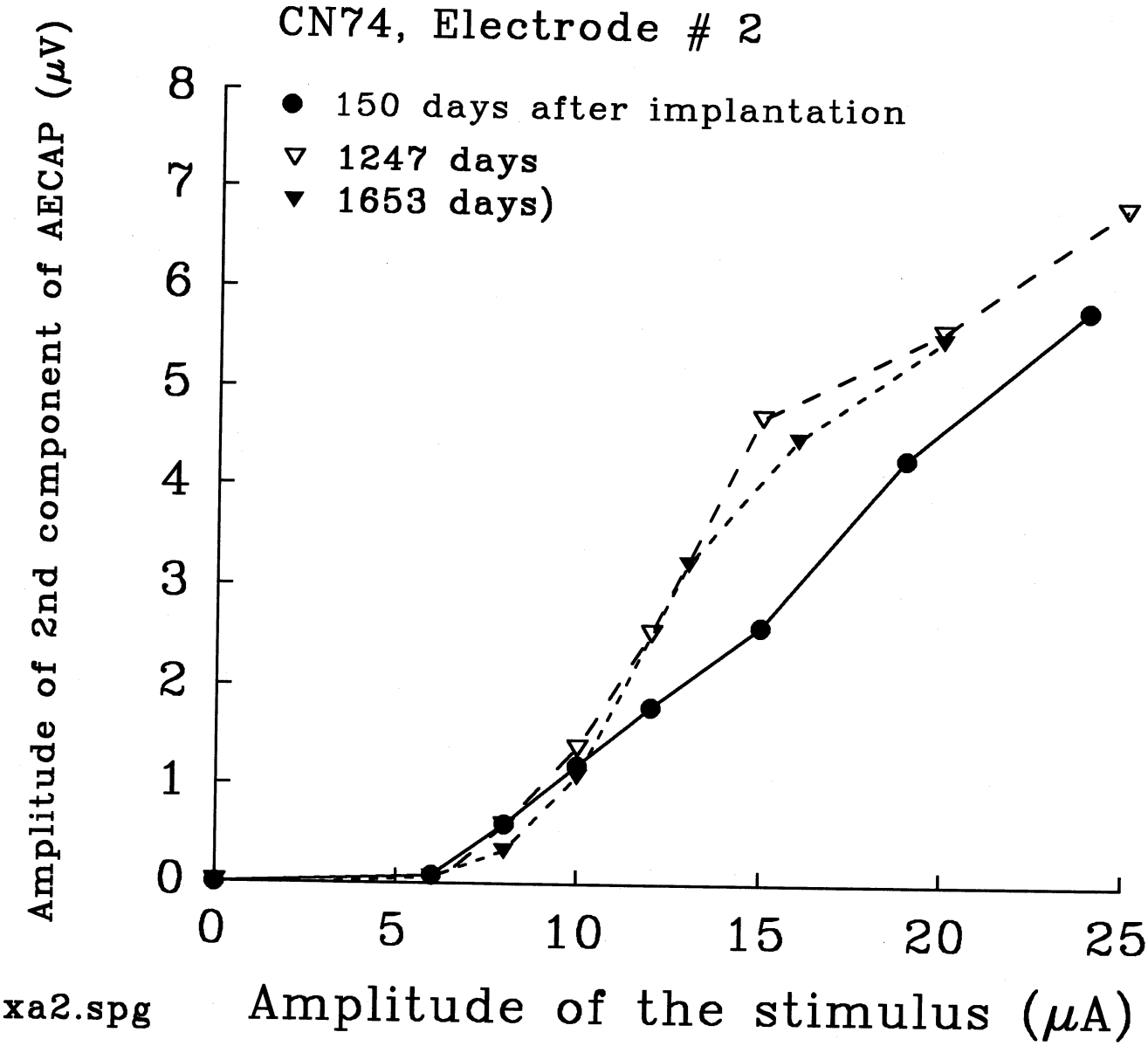

cn74xa2.spg

Figure 13B